J. Biochem. **140**, 457–466 (2006)
doi:10.1093/jb/mvj176

Crystal Structure of *Anti*-Configuration of Indomethacin and Leukotriene B_4 12-Hydroxydehydrogenase/15-Oxo-Prostaglandin 13-Reductase Complex Reveals the Structural Basis of Broad Spectrum Indomethacin Efficacy

Tetsuya Hori[1], Jun Ishijima[1], Takehiko Yokomizo[2,3], Hideo Ago[1], Takao Shimizu[2] and Masashi Miyano[1,*]

[1]Structural Biophysics Laboratory, RIKEN SPring-8 Center, Harima Institute, 1-1-1 Kouto, Sayo-cho, Sayo-gun, Hyogo 679-5148; and [2]Department of Biochemistry and Molecular Biology, Faculty of Medicine, University of Tokyo, and [3]Core Research for Evolutional Science and Technology of Japan Science and Technology Agency, Hongo 7-3-1, Bunkyo-ku, Tokyo 113–0033

Received June 23, 2006; accepted August 10, 2006

The crystal structure of the ternary complex of leukotriene B_4 12-hydroxydehydrogenase/15-oxo-prostaglandin (15-oxo-PG) 13-reductase (LTB_4 12HD/PGR), an essential enzyme for eicosanoid inactivation pathways, with indomethacin and $NADP^+$ has been solved. An indomethacin molecule bound in the *anti*-configuration at one of the two active site clefts of the homo-dimer interface in the LTB_4 12HD/PGR and was confirmed by a binding calorimetry. The chlorobenzene ring is buried in the hydrophobic pore used as a binding site by the ω-chain of 15-oxo-PGE_2. The carboxyl group interacts with the guanidino group of Arg56 and the phenolic hydroxyl group of Tyr262. Indomethacin shows a broad spectrum of efficacy against lipid-mediator related proteins including cyclooxygenase-2, phospholipase A_2, PGF synthase and PGE synthase-2 but in the *syn*-configuration as well as LTB_4 12HD/PGR in the *anti*-configuration. Indomethacin does not necessarily mimic the binding mode of the lipid-mediator substrates in the active sites of these complex structures. Thus, the broad spectrum of indomethacin efficacy can be attributed to its ability to adopt a range of different stable conformations. This allows the indomethacin to adapt to the distinct binding site features of each protein whilst maintaining favorable interactions between the carboxyl group and a counter charged functional group.

Key words: crystal structure, indomethacin, inhibition mechanism, isothermal titration calorimetry, leukotriene B_4 12-hydroxydehydrogenase/15-oxo-prostaglandin 13-reductase.

Abbreviations: COX, cyclooxygenase; indomethacin, [1-(4-chlorobenzoyl)-5-methoxy-2-methyl-1*H*-indole-3-acetic acid]; ITC, isothermal titration calorimetry; LTB_4 12HD/PGR, leukotriene B_4 12-hydroxydehydrogenase/15-oxo-prostaglandin 13-reductase; mPGES-2, microsomal prostaglandin E synthase type 2; PGFS, prostaglandin $F_{2\alpha}$ synthase; PLA_2, phospholipase A_2.

Indomethacin [1-(4-chlorobenzoyl)-5-methoxy-2-methyl-1*H*-indole-3-acetic acid] is a highly effective analgesic drug and one of the "classical" non-steroidal anti-inflammatory drugs (NSAIDs) in common usage (*1*, *2*) (Fig. 1A). The effect of the drug is primarily attributed to the non-selective inhibition of cyclooxygenase 1 and 2 (COX-1 and -2) activity, resulting in decreased production of prostaglandins (PGs), lipid-mediators for inflammation (*3*). Indomethacin also modulates a wide range of enzymes and receptors other than COXs (*4–11*), with effects not limited to inflammation and pain regulation (*4–6*). For example, indomethacin and other several NSAIDs reduce the amyloid-β42 level, whose toxic aggregation is one of the initial pathological steps in Alzheimer's disease. This activity is independent of COX inhibitory activity, although a target protein remains to be identified (*4*). Indomethacin also acts as an agonist to peroxisome proliferator-activated receptor γ (PPARγ), which is highly expressed in adipocytes and induces adipocyte differentiation (*5*). In addition, indomethacin and several NSAIDs induce NSAID-activated gene 1 (NAG-1), a member of the transforming growth factor β (TGF-β) superfamily, which possesses proapoptotic and antitumorigenic effects independent of COX activity in some cells (*6*). Furthermore, indomethacin inhibits leukotriene B_4 12-hydroxydehydrogenase/15-oxo-prostaglandin 13-reductase (LTB_4 12HD/PGR), in the eicosanoid inactivation pathway (*7*), prostaglandin $F_{2\alpha}$ synthase (PGFS, referred to as an aldo-ketoreductase AKR1C3) (*8*) and microsomal PGE synthase type 2 (mPGES-2) (*9*). The pathophysiological relevance of the actions of indomethacin on these enzymes is not known. Indomethacin is also an antagonist of PPARδ (*10*) and an agonist of CRTH2 (chemoattractant receptor–homologous molecule expressed on T-helper type 2 cells), a rhodopsin family G-protein coupled receptor acting as a PGD_2 receptor (DP2) (*11*). Most of the target proteins of

*To whom correspondence should be addressed. Tel: +81-791-58-2815, Fax: +81-791-58-2816, E-mail: miyano@spring8.or.jp

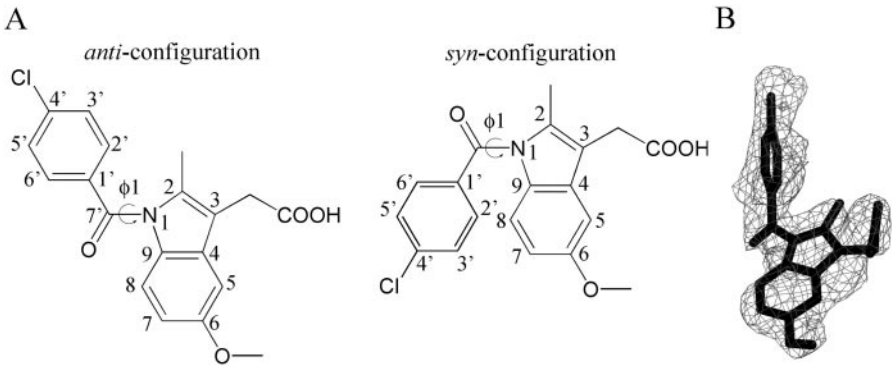

Fig. 1. **Indomethacin structure.** (A) Schematic drawing of the chemical structure of the *anti*- and *syn*-configurations of indomethacin. The atom numbers are defined according to the formal name of indomethacin, [1-(4-chlorobenzoyl)-5-methoxy-2-methyl-1*H*-indole-3-acetic acid]. The ϕ1 axis is defined as the dihedral angle of C9-N1-C7'-C1'. (B) The $|F_o| - |F_c|$ simulated annealing omit map contoured at 3.3 σ of the final indomethacin model.

indomethacin are lipid-mediator related proteins. In order to understand the molecular basis of the broad spectrum of activities of indomethacin and facilitate the design of more effective drugs with fewer side effects it is necessary to obtain structural detail on the different indomethacin binding modes. We have examined the binding mode of indomethacin to LTB_4 12HD/PGR and compared this with the binding modes to other lipid-mediator related target proteins.

The bi-functional LTB_4 12HD/PGR is expressed in various tissues in mammals (*12*) and is induced by a cancer drug dithiolethione (*13*). LTB_4 12HD/PGR is responsible for the regulation of clearance of lipid mediators, catalyzing the first irreversible reaction in the pathway to inactivate various types of lipid mediators (*14–17*). LTB_4 12HD/PGR catalyzes the $NAD(P)^+$ dependent oxidation of LTB_4 to inactive 12-oxo-LTB_4 (*14*). LTB_4 12HD/PGR also irreversibly catalyzes the NAD(P)H dependent reduction of various 15-oxo-PGs and 15-oxo-lipoxin A_4 (LXA_4) to 13,14-dihydro-15-oxo forms in the clearance pathways of relatively stable E and F series of PGs and LXA_4. (*15*, *16*). These lipid-mediators play crucial roles in broad biological responses such as inflammation (reviewed in Ref. *18*). For example, pro-inflammatory LTB_4 leads to the activation and chemotaxis of leukocytes (reviewed in Ref. *19*). Pro-inflammatory PGE_2 is a potent vasodilator in inflammation sites to promoting exudate formation (reviewed in Refs. *18* and *20*). Anti-inflammatory LXA_4 regulates excessive leukocyte traffic, down-regulates leukocyte function and promotes resolution of inflammation (*21*). The inhibition of LTB_4 12HD/PGR by NSAIDs also affects the complex inflammation balance, since LTB_4 12HD/PGR is responsible for the regulation of clearance of these lipid-mediators.

LTB_4 12HD/PGR structure has a typical medium-chain dehydrogenase fold (*17*). The homo-dimer protein is in two-fold symmetry with the two active sites at the dimer interface. In the ternary complex structure with 15-oxo-PGE_2 and $NADP^+$, both active sites were occupied by 15-oxo-PGE_2 and $NADP^+$. The ω-chain moieties of both bound 15-oxo-PGE_2 molecules were buried in the hydrophobic pores of the two active sites, whereas the α-chains are exposed to the solvent (*17*).

Here we report the crystal structure of the ternary complex of LTB_4 12HD/PGR with $NADP^+$ and indomethacin. The bound indomethacin in the *anti*-configuration of the chlorobenzene and indole rings is accommodated into only one of the two substrate binding sites of LTB_4 12HD/PGR. This is the first observation of an *anti*-configuration of bound indomethacin in protein; all the other protein-indomethacin complexes report a *syn*-configuration (Fig. 1A). The broad efficacy of indomethacin is attributed to the flexibility of the molecule allowing dramatic changes in conformation. This structural flexibility allows indomethacin to adapt to the various features of the binding site whilst maintaining a favor interaction between the carboxyl group of indomethacin and polar groups in the many target proteins.

EXPERIMENTAL PROCEDURES

Expression, Purification and Crystallization—All procedures of expression, purification and crystallization were performed as previously described (*12*, *17*). Briefly, guinea-pig LTB_4 12HD/PGR was expressed as a GST fusion protein in *Escherichia coli* strain BL21 Star™ (DE3) cells (Invitrogen) at 20°C. GST-LTB_4 12HD/PGR was purified on a Glutathione Sepharose 4B column (GE Healthcare Bio-Science), and the N-terminal GST was removed with thrombin (Wako), followed by further purification on a Mono S column (GE Healthcare Bio-Science). The buffer was exchanged to 20 mM Tris-HCl (pH 8.0), 150 mM NaCl and 1 mM DTT using a desalting column (GE Healthcare Bio-Science), and the sample was concentrated to 1 mg/ml by ultra-filtration (Millipore). Ten mM $NADP^+$ (Sigma) and 3 mM indomethacin (Cayman chemical) were added to the protein sample followed by incubation for 30 min at room temperature. The protein complex sample was then further concentrated to 20 mg protein/ml. Crystals were obtained using the oil-batch method by mixing equal volumes of protein and precipitant solution [100 mM 4-morpholineethanesulfonic acid (MES) (pH 6.4), 20 to 30% polyethylene glycol 4,000 and 50 mM $MgCl_2$] at 20°C. The same condition yielded crystals of LTB_4 12HD/PGR complexed with 15-oxo-PGE_2 and $NADP^+$ or with $NADP^+$ only (*17*). Crystals appeared within 1 week.

Table 1. **Data collection and structural refinement statistics.**

Beam line	BL45XU (Jupiter CCD)
Space group	Monoclinic $P2_1$
Unit cell *a, b, c* (Å) and β (°)	58.3, 76.1, 79.6 and 102.6
Resolution (Å)	34.2–2.0 (2.07–2.00 Å)[a]
Wavelength (Å)	1.0000
No. of observed ref.	325,829
Unique ref.	45,006
Completeness (%)	97.9 (84.1)
$\langle I/\sigma \rangle$	51.9 (10.8)
R_{merge} (%)	7.0 (17.9)
R_{cryst} (%)	18.1
R_{free} (%)[b]	22.4
r.m.s. deviation	
Bonds (Å)	0.007
Angles (°)	1.12
No. of amino acids in asymmetric unit[c]	664
No. of waters in asymmetric unit	600
Average *B*-factor (Å^2)	
All	31.7
Indomethacin	58.3
NADP in each monomer	23.4/18.7
Tris	45.9

[a]Numbers in parentheses are the values in the highest resolution shell (2.07–2.00 Å). [b]R_{free} is calculated for 5% of data omitted from refinement calculations. [c]It includes residual thrombin recognition sites.

Data Collection and Structural Analysis—X-ray diffraction data were collected at 100 K at RIKEN Structural Biology Beamline I (BL45XU) at SPring-8 (*22*) with a Jupiter CCD detector (RIGAKU) (Table 1). For cryo-cooling, the crystal was treated with a 1:1 Paraffin/Paratone-N mixture (Hampton Research). The data were processed using HKL2000 (*23*), and the refinement of the structure was initiated with the rigid-body refinement in CNS (*24*) using the atomic coordinates of the LTB_4 12HD/PGR and $NADP^+$ binary complex structure (PDB id: 1V3T) (*17*). The atomic coordinate of indomethacin was derived from the crystal structure of iodo-indomethacin (*25*) and was energy minimized with QUANTA/CHARMm (Accelrys). The iterative model re-building and the refinement of the ternary complex were performed using O (*26*), CNS (*24*) and REFMAC5 with TLS refinement (*27*). One homo-dimer of LTB_4 12HD/PGR, one indomethacin, two $NADP^+$, one Tris molecules as well as 600 waters exist per asymmetric unit in the space group $P2_1$. The electron density of indomethacin was well defined (Fig. 1B). The whole 15-oxo-PGE_2 bound molecule was modeled into the structure of the 15-oxo-PGE_2, $NADP^+$ and LTB_4 12HD/PGR ternary complex (PDB id: 1V3V), since the electron density of only the ω-chain had been defined (*17*). Three LTB_4 12HD/PGR structures (indomethacin and $NADP^+$ ternary; PDB id: 2DM6, 15-oxo-PGE_2 and $NADP^+$ ternary; 1V3V and $NADP^+$ binary complexes; 1V3T) were crystallized under the same conditions. The unit cell dimensions and space group were identical for all the crystals allowing an analysis of the structural changes without consideration of the effect of crystal packing (*17*). The figures were prepared with MolScript (*28*), Bobscript (*29*), Raster3D (*30*) and QUANTA/CHARMm (Accelrys).

Isothermal Titration Calorimetry—Isothermal titration calorimetry (ITC) experiments were performed at 37°C using a VP-ITC microcalorimeter (MicroCal). LTB_4 12HD/PGR was dialyzed against 0.1 M sodium phosphate buffer (pH 7.4) containing 1 mM 2-mercaproethanol (buffer A) overnight. Both the enzyme solution (69.7 μM LTB_4 12HD/PGR and 1 mM NADH in buffer A) and the ligand solution (1.5 mM indomethacin and 1 mM NADH in buffer A) were degassed *in vacuo* for 3 min at 30°C prior to use. Heat effects were recorded as a function of time with 10 μl injections of the ligand solution into the sample cell containing the enzyme solution. Data were analyzed using the ITC data analysis module in Origin 5.0 (MicroCal) to determine the binding constant (K_d), binding enthalpy (ΔH), and stoichiometry (n). The titration curve fitted well to a model of "a single set of sites." The entropy (ΔS) and free energy (ΔG) changes were evaluated using the following equation,

$$\Delta G = RT \ln K_d = \Delta H - T\Delta S$$

where R and T are the gas constant and the absolute temperature, respectively.

Enzyme Assays—Inhibition of PGR activity by indomethacin was assayed by the chromophore method as described (*17*). Briefly, the reaction was initiated by incubating 100 μl of enzyme-cofactor complex (1 mM NADH and 0.5 μg enzyme) and 100 μl of substrate-indomethacin mixture (100 μM 15-oxo-PGE_2 and various concentration of indomethacin) in buffer for 0 or 5 min at 37°C. The reaction was terminated by addition of 400 μl of methanol. Then, 600 μl of 2 N NaOH was added to measure the amount of remaining 15-oxo-PGE_2 by reading the maximal absorption at 500 nm using a time course mode of a UV-visible spectrophotometer MultiSpec-2100 (Shimadzu, Japan). The IC_{50} value was calculated using Prism4 (GraphPad).

RESULTS

Indomethacin Binding to LTB_4 12HD/PGR—The thermodynamic parameters for the binding of indomethacin to the LTB_4 12HD/PGR and NADH complex were measured by ITC revealing a favorable, exothermic interaction (Fig. 2). The large negative value of ΔH (–20.2 ± 2.28 kcal/mol or –84.5 ± 9.54 J/mol) compensated the decrease in entropy ($T\Delta S$ = –14.8 kcal/mol or –61.9 J/mol), resulting in a substantial negative ΔG (–5.4 kcal/mol, –22.6 J/mol) at 37°C. The decrease in entropy suggested to occur a certain conformational restraints by the NADH and indomethacin complex formation in LTB_4 12HD/PGR. Stoichiometry of indomethacin binding per one active site of LTB_4 12HD/PGR was calculated to be 0.58 ± 0.059. This is consistent with the result of the crystallographic studies, showing that only one active site was occupied by an indomethacin molecule in the LTB_4 12HD/PGR homodimer structure as described below. In contrast the substrate 15-oxo-PGE_2 is defined in both active sites of the ternary LTB_4 12HD/PGR homodimer structure complexed with 15-oxo-PGE_2 and $NADP^+$ (*17*).

The IC_{50} of indomethacin on 15-oxo-PGE_2 reductase activity of LTB_4 12HD/PGR (97.9 ± 19.4 μM) is compatible with that of the dissociation constant (K_d = 159.2 μM) obtained by ITC (Fig. 2).

Structure of the Indomethacin Binding Site—In the crystal structure of the LTB_4 12HD/PGR complex, the

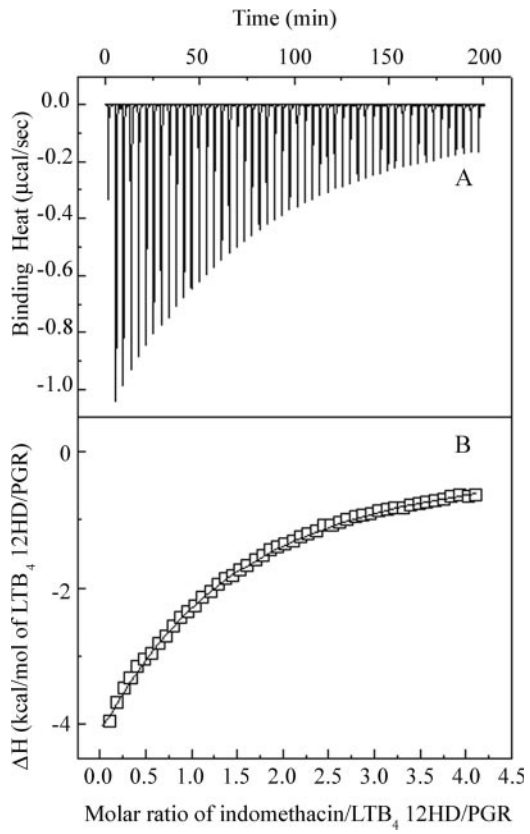

Fig. 2. **Isothermal titration calorimetry of indomethacin binding to LTB_4 12HD/PGR at 37°C.** (A) The heat release with the titration for the association using 69.7 μM LTB_4 12HD/PGR monitored by ITC. (B) Integration of the thermogram yielded a binding isotherm (open squares) that fits to the model (solid line). K_d = 159.2 μM, ΔG = –5.4 kcal/mol, ΔH = –20.2 ± 2.28 kcal/mol, $T\Delta S$ = –14.8 kcal/mol at 37°C and n = 0.58 ± 0.059.

bound indomethacin is located next to the nicotineamide ring of $NADP^+$ in only one of the two active sites of LTB_4 12HD/PGR (Fig. 3A). The bound indomethacin occupies one of the same binding sites occupied by 15-oxo-PGE_2 in the substrate binding complex (Fig. 4A). The carboxyl group of the bound indomethacin makes a salt bridge with the guanidino group of Arg56 (over a distance of 2.8 Å) from one monomer (termed monomer 1) and a hydrogen bond with the phenolic hydroxyl group of Tyr262 (over a distance of 2.6 Å) from the other monomer (monomer 2) at the dimer interface of the substrate binding pore (Fig. 3A). The positive electrostatic potential around Arg56 and Tyr262 is complimentary to the negatively charged carboxyl group of the bound indomethacin with the salt bridge forming with Arg56 (Fig. 3, B and C).

The chlorobenzene ring of the bound indomethacin is buried in the hydrophobic pore at the dimer interface of the LTB_4 12HD/PGR monomers (Fig. 3, A and B), where the ω-chain of 15-oxo-PGE_2 binds in the complex structure (Fig. 4A). The residues surrounding the chlorobenzene ring and within 4 Å are Tyr245 from monomer 1, and Pro257, Glu258, Ile261 and Tyr262 from monomer 2 (Fig. 3A). The plane of the chlorobenzene ring is about 60° from that of the phenyl ring of Tyr262 and the two groups form an aromatic-aromatic interaction (*31*). In addition, the phenolic hydroxyl group of Tyr245 makes a weak hydrogen bond with the benzene ring hydrogen with a short atomic distance of the hydroxyl oxygen atom to the C3′ atom of the chlorobenzene of 3.0 Å (*32*), contributing to the stabilization of the indomethacin binding (Fig. 3A). There are no water molecules in the indomethacin bound pore.

In contrast to the chlorobenzene ring, the indole ring of the bound indomethacin is accessible to solvent in the complex structure of LTB_4 12HD/PGR (Fig. 3B). There is no direct interaction between the indole ring and the nicotineamide ring of $NADP^+$, since there are three water molecules (W1–W3) between the two rings (Fig. 3A). The bound water, W1 has been proposed to be a catalytic water indispensable for the 15-oxo-PGE_2 reductase reaction due to its stabilizing effect on the enolate anion intermediate (*17*). W1 was also found in all the structures of the $NADP^+$ and LTB_4 12HD/PGR complex, regardless of 15-oxo-PGE_2 or indomethacin binding (*17*). At the solvent region, the oxygen atom of the methoxy group of indomethacin makes a hydrogen bond with the water W4 (over a distance of 2.8 Å). These results indicate that the amphipathic indomethacin is highly suited for binding to LTB_4 12HD/PGR, since the hydrophobic portion of the molecule is surrounded by the hydrophobic pore of LTB_4 12HD/PGR and the negatively charged carboxyl group interacts with the positively charged Arg56 and Tyr262 residues. The bound form of indomethacin is in the *anti*-configuration (Fig. 3A) with the torsion angle around C9-N1-C7'-C1' (ϕ1) of 144° (Fig. 1A).

Structural Changes in LTB_4 12HD/PGR Induced by Indomethacin Binding—Indomethacin binding induces a structural change in the active site due to van der Waals repulsion (Fig. 4A). When the indomethacin or 15-oxo-PGE_2 bound complex structures (PDB id: 2DM6 and 1V3V, respectively) were superimposed at one monomer (monomer 2) of the LTB_4 12HD/PGR homo-dimer, several residues of the 15-oxo-PGE_2 binding complex, Tyr49, Ala53 and Ile271 in monomer 1 and Tyr262 in monomer 2, are located within the distances of the van der Waals radii of the indomethacin molecule in the indomethacin bound complex structure (Fig. 4A). These steric hindrances result in distortion of the active site at the border of the two monomers which causes formation of the wider hydrophobic pore of the substrate binding site observed in the indomethacin bound complex compared to the 15-oxo-PGE_2 bound form (Fig. 4A). In the superimposed LTB_4 12HD/PGR structures using only the monomer 2 subunits, the differences of the corresponding Cα atom positions are 1.7, 1.7 and 1.0 Å in Tyr49, Ala53 and Ile271 residues from monomer 1, respectively, and 0.7 Å in Tyr262 from monomer 2 in the indomethacin occupied active site, whereas the corresponding distances are 0.2, 0.2, 0.5 and 0.6 Å in the indomethacin unbound active site, respectively. Thus, the region of the protein involved in forming the indomethacin bound active site was substantially distorted in order to accommodate the bulkier indomethacin molecule.

The distortion of the indomethacin bound active site also results in a rigid-body rotation of the monomer (Fig. 4, A and B). When the indomethacin and 15-oxo-PGE_2 binding complex structures were superimposed at monomer 2, the r.m.s. deviation for all Cα atoms in monomer 2 is 0.9 Å while for monomer 1 the r.m.s. deviation is 2.2 Å.

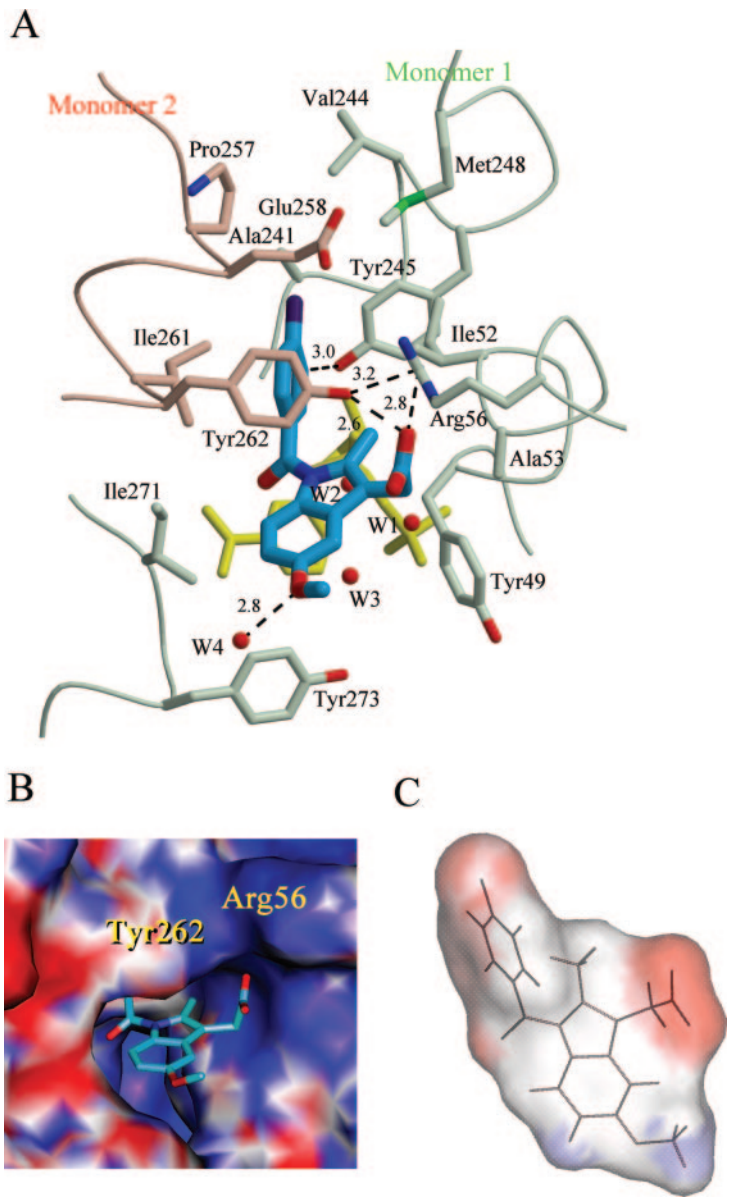

Fig. 3. **The binding mode of indomethacin to the dimer interface of LTB_4 12HD/PGR.** (A) The indomethacin binding structure. Indomethacin, a nicotineamide moiety of $NADP^+$ (all atoms colored in yellow), bound waters W1–W4 and surrounding residues are shown. The carbon atoms of indomethacin are in cyan. The carbon atoms of residues from monomer 1 are colored in light green and those of monomer 2 are in light pink. The nitrogen, oxygen, chloride and sulfur atoms are colored in blue, red, indigo and green, respectively. The salt bridge and hydrogen bonds with indomethacin are indicated by dashed lines with distances (Å). (B) Electrostatic potential of the molecular surface of the LTB_4 12HD/PGR active site. Negative and positive potentials are colored in red and blue, respectively. The bound indomethacin is also shown. (C) Electrostatic potential of the molecular surface of bound indomethacin colored as for (B). The electrostatic potentials were calculated by QUANTA/CHARMm (Accelrys) for the active site of LTB_4 12HD/PGR including polar hydrogens (B) and for the bound indomethacin including all hydrogens (C).

Compared with the position of center of mass for each monomer, the conformational change corresponds to monomer 1 rotation by 6° (Fig. 4B). However such rigid-body rotation was not observed between the structures with and without bound 15-oxo-PGE_2, and the r.m.s. deviation of 0.5 Å for the whole dimeric structures was observed (PDB id: 1V3V and 1V3T) (*17*). The slight structural change induced around the active site by the asymmetric binding of indomethacin causes the monomer rotation which prevents a second indomethacin or 15-oxo-PGE_2 from occupying the vacant active site.

When the indomethacin or 15-oxo-PGE_2 binding complexes were superimposed at the monomer 2, whose active site was vacant in the indomethacin bound complex, it was observed that the residues around the vacant active site, especially Ile242 to Pro253, slightly shift to close the cavity. Since both the active sites are adjacent with non-crystallographic two fold symmetry in dimer, those residues lined in the vacant active site should be sterically strained due to the structural change of the indomethacin occupied active site by the bound indomethacin in the monomer 1. The structural shift would be the counter direction as expected when an indomethacin molecule bound to the vacant active site, resulting in prohibiting additional indomethacin binding. The implication for the vacant active site based on the indomethacin complex structure is compatible with the binding stoichiometry (n = 0.58 ± 0.059) and the large decrease of entropy ($T\Delta S$ = –14.8 kcal/mol at 37°C) by indomethacin binding to the active site of LTB_4 12HD/PGR in solution (Fig. 2). The structural constraints on the vacant active site due to monomer rotation also inhibits binding of the substrate, 15-oxo-PGE_2. The lack of structural change induced in the second active site upon 15-oxo-PGE_2 binding may be the reason why both active sites can be occupied in the 15-oxo-PGE_2 bound form (*17*). In summary, the bulk indomethacin binds to only one of the two 15-oxo-PGE_2 binding sites in the homo-dimer of LTB_4 12HD/PGR. Indomethacin

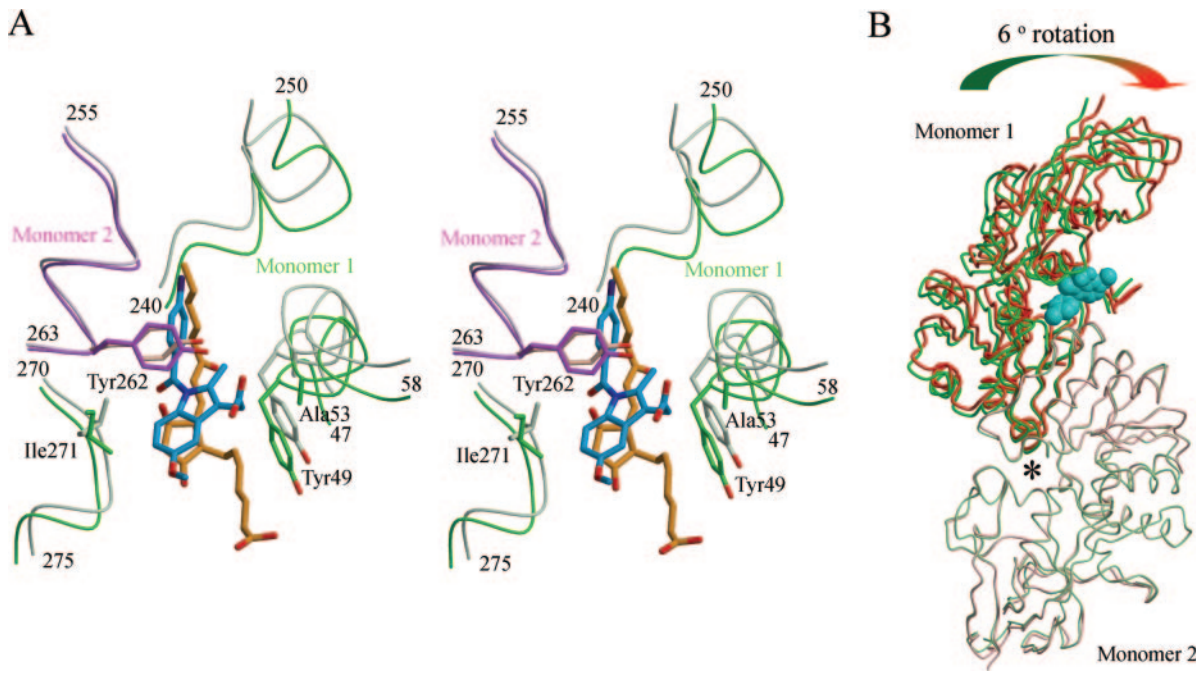

Fig. 4. **Superposition of LTB_4 12HD/PGR structure with indomethacin and $NADP^+$, and 15-oxo-PGE_2 and $NADP^+$.** Only one monomer (monomer 2) of each complex was used for the superposition. (A) The stereo view of the superposition around the indomethacin bound active site. The indomethacin binding complex structure is colored in green (monomer 1) and magenta (monomer 2), and the 15-oxo-PGE_2 binding complex model is in light-green (monomer 1) and light-magenta (monomer 2). The carbon atoms of the indomethacin and 15-oxo-PGE_2 are colored in cyan and orange, respectively. (B) Over view of the superposition. Indomethacin binding complex is colored in green (monomer 1) and light-green (monomer 2), and 15-oxo-PGE_2 binding complex model is in red (monomer 1) and light-red (monomer 2). The bound indomethacin is colored in cyan and the indomethacin unbound active site is indicated by an asterisk.

binding induces monomer rotation and the resultant structural constraints imposed prevent binding to the second site.

DISCUSSION

This paper describes the first structure of LTB_4 12HD/PGR in complex with bound indomethacin which has revealed that indomethacin binds in the *anti*-configuration of the chlorobenzene and indole rings (Fig. 1A). This is in contrast to the *syn*-configuration observed for indomethacin when bound to other enzymes (*9*, *33*, *34*) (Fig. 1A). Such a flexible nature allows dramatic changes in the conformation of the indomethacin molecule allowing optimal binding to a wide range of proteins. Here we compare the binding modes of indomethacin to a wide angle of enzymes in order to elucidate the structural basis of broad spectrum indomethacin efficacy.

Comparison of the Bound Indomethacin Configurations among Enzymes—The indole and chlorobenzene rings of the bound indomethacin molecule can adopt a number of different conformations dependent on the different characteristics of the binding sites in various enzymes. Indomethacin bound to LTB_4 12HD/PGR has an *anti*-configuration of the flexible imido bond (N1-C7') between the chlorobenzene and indole rings (Fig. 1A), in which the bulky two rings are located in energetically favorable opposite positions (Fig. 1B). The flexible torsion angle of C9-N1-C7'-C1' (ϕ1) is 144°, derived from the steric constraint between the carbonyl oxygen atom and the hydrogen atom attached to C8 (Fig. 1A). Indomethacin bound COX-2 (ϕ1 = –59°) (PDB id: 4COX) (*33*), PGFS (ϕ1 = 44°) (1S2S) (*34*), mPGES-2 (ϕ1 = 22°) (1Z9H) (*9*) and phospholipase A_2 (PLA_2) (ϕ1 = –33°) (1TI0) is in the *syn*-configuration, in which ϕ1 is reversed compared with the *anti*-configuration seen in the LTB_4 12HD/PGR complex (Fig. 5A). Each configuration can be further classified into two sub-classes according to whether the rotation about ϕ1 is clockwise or counterclockwise (Table 2 and Fig. 5). There are four possible stable configurations of the bound indomethacin molecule which yield the same minimal energies *in vacuo* (Table 2). Indomethacins bound to mPGES-2 and PGFS are in the clockwise *syn*-configuration (*syn*1), and bound to COX-2 and PLA_2 in the counterclockwise *syn*-configuration (*syn*2). Indomethacin bound to LTB_4 12HD/PGR is in the clockwise *anti*-configuration (*anti*1), while the final possible configuration of indomethacin bound to a protein in the counterclockwise *anti*-configuration (*anti*2) has yet to be found experimentally.

These results indicate that the configuration of the bound indomethacin molecule can vary about the ϕ1 axis as well as the positions of the carboxyl and the methoxy groups. Indomethacin can thus adapt to the specific features of a number of protein binding sites in order to optimize the indomethacin-protein interaction.

Comparison of the Indomethacin Binding Mode among Enzymes—Indomethacin binds to each enzyme according to a specific binding mode. The binding mode of indomethacin to LTB_4 12HD/PGR is in part analogous to that of COX-2. In each enzyme, the carboxyl group of

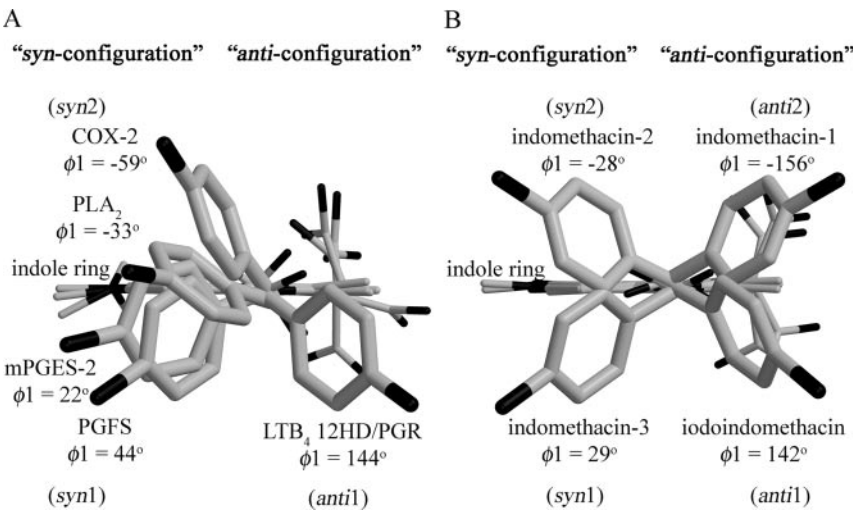

Fig. 5. **Stable configurations of indomethacin.** Indomethacin structures are superimposed with respect to the indole rings and shown parallel to the C7'-N bond defined in Fig. 1A. The chlorobenzene rings are emphasized by the bold sticks. (A) Comparison of the bound indomethacin structures complexed with various lipid-mediator related enzymes; LTB_4 12HD/PGR (PDB id: 2DM6), COX-2 (4COX) (*33*), PGFS (1S2S) (*34*) and PLA_2 (1TL0) and mPGES-2 (1Z9H) (*9*). (B) Crystal structure of indomethacin and iodoindomethacin. The *anti*- and two *syn*-configuration of indomethacins (*anti*2, *syn1* and *syn2*) (CSD reference id: INDMET02) (*42*) and the *anti*-configuration of iodoindomethacin (*anti*1) (HIFYIE) (*25*) (B).

Table 2. **Summary of possible stable configurations and inhibition competence for each enzyme of indomethacin.**

Configuration	Enzyme-indomethacin					Indomethacin single crystal			Calculated[g]
	Enzyme[a]	Complex crystal		Inhibition competence					
		ϕ1[b]	PDB id[c] (ref.)	IC_{50}	(ref.)	Molecule	ϕ1[b]	CSD id[e] (ref.)	ϕ1[b]
syn 1	mPGES-2	22°	1Z9H (*9*)	1 mM	(*9*)	indomethacin	29°	INDMET02[f] (*42*)	43°
	PGFS	44°	1S2S (*34*)	4.1 μM	(*8*)				
syn 2	PLA_2	–33°	1TI0[d]			indomethacin	–28°	INDMET02 (*42*)	–43°
	COX-2	–59°	4COX (*33*)	15 μM	(*36*)				
anti 1	LTB_4 12HD/PGR	144°	2DM6 (This work)	100 μM	(This work)	indomethacin	155°	HIFYIE (*25*)	136°
anti 2						indomethacin	–156°	INDMET02 (*42*)	–138°

[a]Abbreviations: mPGES-2: microsomal prostaglandin E synthase type 2, PGFS: prostaglandin $F_{2\alpha}$ synthase, PLA_2: phospholipase A_2, COX-2: cyclooxygenase-2, LTB_4 12HD/PGR: leukotriene B_4 12-hydroxydehydrogenase/15-oxo-prostaglandin 13-reductase. [b]ϕ1: Torsion angle of C9-N1-C7'-C1' (Fig. 1). [c]PDB: Protein Data Bank (http://www.rcsd.org). [d]Snigh, N. *et al*. (unpublished in PDB). [e]CSD: Cambridge Structural Database. [f]There are three indomethacin molecules in an asymmetric unit. [g]Each indomethacin structure was energy-minimized with QUANTA/CHARMm (Accelrys).

indomethacin forms an interaction with the guanidino group of an arginine and the phenolic hydroxyl group of a tyrosine, Arg56 and Tyr262 of LTB_4 12HD/PGR (Fig. 6A) and Arg120 and Tyr355 of COX-2 (*33*) (Fig. 6B). The chlorobenzene ring of indomethacin in each enzyme is surrounded by hydrophobic residues, which constitute the ω-chain recognition site for 15-oxo-PGE_2 in LTB_4 12HD/PGR (*17*) (Fig. 3A) and are also involved in recognition of the unsaturated hydrocarbon chain of arachidonic acid close to the active site in COX-2 (*35*). However, the most prominent difference in indomethacin binding is in the environment of the indole ring. In LTB_4 12HD/PGR, the indole ring is accessible to the solvent (Fig. 3B). In contrast in COX-2 the indole is surrounded by several hydrophobic residues and is inaccessible to the solvent (*33*).

The binding of indomethacin to other enzymes also varies. In mPGES-2 the chlorobenzene ring is buried in the hydrophobic pocket, while the indole ring is accessible to solvent as in the LTB_4 12HD/PGR-indomethacin complex structure (*9*). In mPGES-2 the carboxyl group of indomethacin forms hydrogen bonds with a thiol group of cysteine and a bound water (*9*). In contrast, in PGFS the bound indomethacin is located inside the hydrophobic cavity of the protein and is totally inaccessible as seen in the COX2-indomethacin complex (*33*, *34*). The carboxyl group of the indomethacin interacts with the oxygen atoms of phospho-diester bond in $NADP^+$, the back-bone nitrogen atom of Gln222 and bound water molecules in the hydrophobic environment (Fig. 6C) (*34*). In snake venom PLA_2 the indomethacin adsorbs on the hydrophobic wall of the active site and one complete side of the indomethacin surface including the chlorobenzene ring is accessible to solvent. In this case the putatively protonated carboxyl group interacts with a carboxyl group of aspartate residue and surrounding water molecules. These complex structures show that the indomethacin binding mode differs according to the protein in terms of some distinct binding site features.

The inhibition competence of indomethacin can be determined according to the environment of the interaction of the carboxyl group of indomethacin with a protein. In pharmacological studies, COX-2 (IC_{50} = 15 μM for pre-incubated indomethacin) (*36*) and PGFS (IC_{50} = 4.1 μM) (*8*) are more competently inhibited by indomethacin than LTB_4 12HD/PGR (IC_{50} = 100 μM) and mPGES-2 (IC_{50} = 1 mM) (*9*). The inhibitory competence of indomethacin is associated with the binding mode of indomethacin and strict inhibition is achieved when indomethacin is fully buried within the hydrophobic cavity of the protein interior. The polar interaction between the carboxyl group

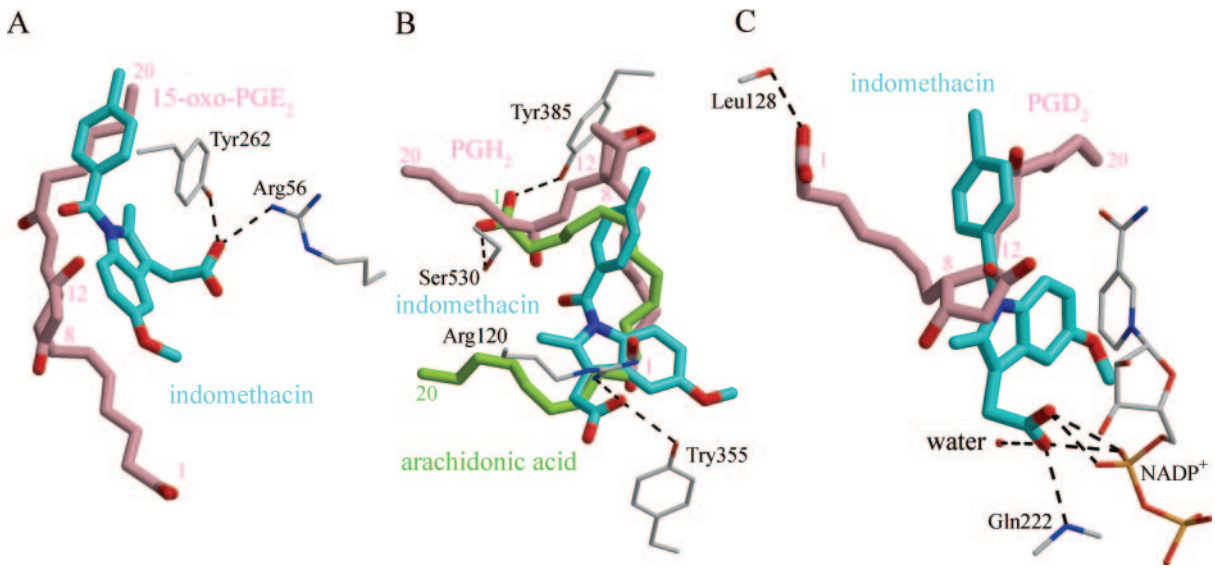

Fig. 6. **Comparison of the binding mode of indomethacin and in the cognate prostanoid for each enzyme.** (A) LTB_4 12HD/PGR (PDB id; 1V3V and 2DM6) (*17*), (B) COX-2 (4COX, 1CVU and 1DDX) (*33*, *35*) and (C) PGFS (1S2A and 1RY0) (*34*, *40*). The indomethacin, substrate or product bound complex structures are superimposed in each enzyme, and the bound ligands and the functional groups interacting with the carboxyl group of the ligands are only represented. The non-bonding interactions are indicated by dashed lines. The carbon atoms of indomethacin, prostaglandins, arachidonic acid and the functional groups of enzymes are colored in cyan, pink, yellow-green and gray, respectively. The carbon atom numbers of prostaglandins and arachidonic acid are indicated. The α-chain and head group of the 15-oxo-PGE_2 was modeled in the ternary complex structure of LTB_4 12HD/PGR with 15-oxo-PGE_2 and $NADP^+$ in which the electron density of only the ω-chain of 15-oxo-PGE_2 had been defined (PDB id: 1V3V) (*17*). In COX-2, the bound arachidonic acid is in a non-productive binding mode (*35*).

of indomethacin and the charged group in the hydrophobic environment as seen in COX-2 (Fig. 6B) (*33*) and PGFS (Fig. 6C) (*34*) contributes to the tighter binding of indomethacin due to lower dielectric constants at the hydrophobic interior of the protein compared to the higher dielectric constants found at the solvent accessible environment as seen in the LTB_4 12HD/PGR (Fig. 6A) and mPGES-2 structures (*9*). Indeed, the interaction with the carboxyl group is indispensable for indomethacin binding to COXs, since mutation of Arg120 in both COX-1 and COX-2 drastically weakened the inhibition by indomethacin (*37*, *38*) and amide and ester derivatives of the carboxyl group of indomethacin have been shown to be inactive for COX-1 inhibition (*39*). These results indicate that the interaction of the carboxyl group of indomethacin with polar groups of a protein is a primary determinant for the inhibitory competence of indomethacin, and the optimum interaction can be obtained through adaptation of the flexible indomethacin configuration.

Comparison of the Binding Mode of Indomethacin and Substrate—Indomethacin binding modes are very different to those of the prostanoid substrates. For LTB_4 12HD/PGR, COX-2 and PGFS, both the indomethacin and substrate complex structures have been determined. Thus it was possible to analyze the binding mode of indomethacin in comparison with that of each bound substrate in order to elucidate whether the indomethacin mimics the binding mode of the natural substrate by superposition of the indomethacin and the corresponding substrate bound complex structures (Fig. 6). In LTB_4 12HD/PGR, the chlorobenzene ring of bound indomethacin overlaps with the C16-C20 of the alkyl ω-chain in the bound 15-oxo-PGE_2, when monomer 2 of the LTB_4 12HD/PGR/$NADP^+$/indomethacin ternary complex structure is superimposed with the ternary complex structure with 15-oxo-PGE_2 and $NADP^+$ (Fig. 6A). In COX-2, the bound indomethacin corresponds to the α-chain (C1-C8) of the PGH_2 complex structure or C5-C14 of the alkyl chain in the arachidonic acid complex structure (Fig. 6B) (*33*, *35*). In PGFS, only the C12-C15 alkyl ω-chain is superimposed to indomethacin (*34*, *40*) (Fig. 6C). Of the crystallographically defined prostanoid substrates, the arachidonic acid and PGH_2 in COX-2 and PGD_2 in PGFS, the carboxyl groups do not share the same interaction with that of indomethacin (Fig. 6, B and C). These results show that there may be little qualitative correlation between the binding mode of indomethacin and the prostanoid substrates indicating that indomethacin does not act as a substrate mimic.

Broad Spectrum of Indomethacin Efficacy—The broad spectrum of indomethacin efficacy can be explained based on the structural insight obtained from the protein-indomethacin complexes; (a) the carboxyl group of the bound indomethacin can interact with a variety of functional groups of target proteins and (b) the bound configuration of the indomethacin is very flexible about the ϕ1 axis, allowing adaptation to the specific features of the binding site in each target protein whilst maintaining optimum interaction of the carboxyl group as discussed above. The flexible configuration of indomethacin enables it to bind to various proteins in binding modes distinct from those observed for the enzyme substrates.

The data revealed by this study may be useful for the future design of inhibitors. Indeed the two phenyl groups of COX-2 selective inhibitors SC58635 and SC558 are fixed in a configuration similar to that of the *syn*-configuration of indomethacin (*33*, *41*). The development of drugs which

mimic the *anti*-configuration of indomethacin may prove to be most effective against LTB_4 12HD/PGR with lower efficacy against COX-2, mPGES-2 or PGFS.

We thank Nobuo Kamiya, Yoshiaki Kawano and Hiroki Nakajima for helping with diffraction data collection at BL45XU. We are grateful to B. Byrne for critical reading of the manuscript. We would like acknowledge Akio Ebihara and Seiki Kuramitsu for the ITC instrument. Data deposition: The atomic coordinates and structure factors have been deposited in the Protein Data Bank, http://www.rcsb.org (PDB codes 2DM6).

REFERENCES

1. Ferreira, S.H., Moncada, S., and Vane, J.R. (1971) Indomethacin and aspirin abolish prostaglandin release from the spleen. *Nat. New. Biol.* **231**, 237–239
2 Smith, W.L. and Lands, W.E. (1971) Stimulation and blockade of prostaglandin biosynthesis. *J. Biol. Chem.* **246**, 6700–6702
3 Hla, T. and Neilson, K. (1992) Human cyclooxygenase-2 cDNA. *Proc. Natl. Acad. Sci. USA* **89**, 7384–7388
4 Weggen, S., Eriksen, J.L., Das, P., Sagi, S.A., Wang, R., Pietrzik, C.U., Findlay, K.A., Smith, T.E., Murphy, M.P., Bulter, T., Kang, D.E., Marquez-Sterling, N., Golde, T.E., and Koo, E.H. (2001) A subset of NSAIDs lower amyloidogenic Aβ42 independently of cyclooxygenase activity. *Nature* **414**, 212–216
5 Lehmann, J.M., Lenhard, J.M., Oliver, B.B., Ringold, G.M., and Kliewer, S.A. (1997) Peroxisome proliferator-activated receptors α and γ are activated by indomethacin and other non-steroidal anti-inflammatory drugs. *J. Biol. Chem.* **272**, 3406–3410
6 Baek, S.J., Kim, K.S., Nixon, J.B., Wilson, L.C., and Eling, T.E. (2001) Cyclooxygenase inhibitors regulate the expression of a TGF-β superfamily member that has proapoptotic and antitumorigenic activities. *Mol. Pharmacol.* **59**, 901–908
7 Clish, C.B., Sun, Y.P., and Serhan, C.N. (2001) Identification of dual cyclooxygenase-eicosanoid oxidoreductase inhibitors: NSAIDs that inhibit PG-LX reductase/LTB_4 dehydrogenase. *Biochem. Biophys. Res. Commun.* **288**, 868–874
8 Matsuura, K., Shiraishi, H., Hara, A., Sato, K., Deyashiki, Y., Ninomiya, M., and Sakai, S. (1998) Identification of a principal mRNA species for human 3α-hydroxysteroid dehydrogenase isoform (AKR1C3) that exhibits high prostaglandin D_2 11-ketoreductase activity. *J. Biochem.* **124**, 940–946
9 Yamada, T., Komoto, J., Watanabe, K., Ohmiya, Y., and Takusagawa, F. (2005) Crystal structure and possible catalytic mechanism of microsomal prostaglandin E synthase type 2 (mPGES-2). *J. Mol. Biol.* **348**, 1163–1176
10 Yu, K., Bayona, W., Kallen, C.B., Harding, H.P., Ravera, C.P., McMahon, G., Brown, M., and Lazar, M.A. (1995) Differential activation of peroxisome proliferator-activated receptors by eicosanoids. *J. Biol. Chem.* **270**, 23975–23983
11 Hirai, H., Tanaka, K., Takano, S., Ichimasa, M., Nakamura, M., and Nagata, K. (2002) Cutting edge: agonistic effect of indomethacin on a prostaglandin D_2 receptor, CRTH2. *J. Immunol.* **168**, 981–985
12 Yamamoto, T., Yokomizo, T., Nakao, A., Izumi, T., and Shimizu, T. (2001) Immunohistochemical localization of guinea-pig leukotriene B_4 12-hydroxydehydrogenase/15-ketoprostaglandin 13-reductase. *Eur. J. Biochem.* **268**, 6105–6113
13 Primiano, T., Li, Y., Kensler, T.W., Trush, M.A., and Sutter, T.R. (1998) Identification of dithiolethione-inducible gene-1 as a leukotriene B_4 12-hydroxydehydrogenase: implications for chemoprevention. *Carcinogenesis* **19**, 999–1005
14 Yokomizo, T., Izumi, T., Takahashi, T., Kasama, T., Kobayashi, Y., Sato, F., Taketani, Y., and Shimizu, T. (1993) Enzymatic inactivation of leukotriene B_4 by a novel enzyme found in the porcine kidney. *J. Biol. Chem.* **268**, 18128–18135
15 Ensor, C.M., Zhang, H., and Tai, H.H. (1998) Purification, cDNA cloning and expression of 15-oxoprostaglandin 13-reductase from pig lung. *Biochem. J.* **330**, 103–108
16 Clish, C.B., Levy, B.D., Chiang, N., Tai, H.H., and Serhan, C.N. (2000) Oxidoreductases in lipoxin A_4 metabolic inactivation. *J. Biol. Chem.* **275**, 25372–25380
17 Hori, T., Yokomizo, T., Ago, H., Sugahara, M., Ueno, G., Yamamoto, M., Kumasaka, T., Shimizu, T., and Miyano, M. (2004) Structural basis of leukotriene B_4 12-hydroxydehydrogenase/15-oxo-prostaglandin 13-reductase catalytic mechanism and a possible Src homology 3 domain binding loop. *J. Biol. Chem.* **279**, 22615–22623
18 Lawrence, T., Willoughby, D.A., and Gilroy, D.W. (2002) Anti-inflammatory lipid mediators and insights into the resolution of inflammation. *Nat. Rev. Immunol.* **2**, 787–795
19 Toda, A., Yokomizo, T., and Shimizu, T. (2002) Leukotriene B_4 receptors. *Prostaglandins Other Lipid Mediat.* **68–69**, 575–585
20 Charlier, C. and Michaux, C. (2003) Dual inhibition of cyclooxygenase-2 (COX-2) and 5-lipoxygenase (5-LOX) as a new strategy to provide safer non-steroidal anti-inflammatory drugs. *Eur. J. Med. Chem.* **38**, 645–659
21 Levy, B.D., Clish, C.B., Schmidt, B., Gronert, K., and Serhan, C.N. (2001) Lipid mediator class switching during acute inflammation: signals in resolution. *Nat. Immunol.* **2**, 612–619
22 Kumasaka, T., Yamamoto, M., Yamashita, E., Moriyama, H., and Ueki, T. (2002) Trichromatic concept optimizes MAD experiments in synchrotron X-ray crystallography. *Structure* **10**, 1205–1210
23 Otwinowski, Z. and Minor, W. (1997) Processing of x-ray diffraction data collected in oscillation mode. *Methods Enzymol.* **276**, 307–326
24 Brunger, A.T., Adams, P.D., Clore, G.M., DeLano, W.L., Gros, P., Grosse-Kunstleve, R.W., Jiang, J.S., Kuszewski, J., Nilges, M., Pannu, N.S., Read, R.J., Rice, L.M., Simonson, T., and Warren, G.L. (1998) Crystallography & NMR system: A new software suite for macromolecular structure determination. *Acta Crystallogr. Sect. D* **54**, 905–921
25 Loll, P.J., Garavito, R.M., Carrell, C.J., and Carrell, H.L. (1996) 1-(4-iodobenzoyl)-5-methoxy-2-methyl-3-indoleacetic acid, an iodinated indomethacin analog. *Acta. Crystallogr. Sect. C* **52**, 455–457
26 Jones, T.A., Zou, J.Y., Cowan, S.W., and Kjeldgaard, M. (1991) Improved methods for building protein models in electron density maps and the location of errors in these models. *Acta Crystallogr. Sect. A* **47**, 110–119
27 Murshudov, G.N., Vagin, A.A., and Dodson, E.J. (1997) Refinement of macromolecular structures by the maximum-likelihood method. *Acta Crystallogr. Sect. D* **53**, 240–255
28 Kraulis, P.J. (1991) MOLSCRIPT: a program to produce both detailed and schematic plots of protein structures. *J. Appl. Crystallogr.* **24**, 946–950
29 Esnouf, R.M. (1997) An extensively modified version of MolScript that includes greatly enhanced coloring capabilities. *J. Mol. Graph.* **15**, 132–134
30 Merrit, E.A. and Bacon, D.J. (1997) Raster 3D: Photorealistic molecular graphics. *Methods Enzymol.* **277**, 505–524
31 Burley, S.K. and Petsko, G.A. (1986) Dimerization energetics of benzene and aromatic amino acid side chains. *J. Am. Chem. Soc.* **108**, 7995–8001
32 Steiner, T. (1997) Unrolling the hydrogen bond properties of C-H···O interactions. *Chem. Commun.* 727–734
33 Kurumbail, R.G., Stevens, A.M., Gierse, J.K., McDonald, J.J., Stegeman, R.A., Pak, J.Y., Gildehaus, D., Miyashiro, J.M., Penning, T.D., Seibert, K., Isakson, P.C., and Stallings, W.C.

(1996) Structural basis for selective inhibition of cyclooxygenase-2 by anti-inflammatory agents. *Nature* **384**, 644–648
34 Lovering, A.L., Ride, J.P., Bunce, C.M., Desmond, J.C., Cummings, S.M., and White, S.A. (2004) Crystal structures of prostaglandin D_2 11-ketoreductase (AKR1C3) in complex with the nonsteroidal anti-inflammatory drugs flufenamic acid and indomethacin. *Cancer Res.* **64**, 1802–1810
35 Kiefer, J.R., Pawlitz, J.L., Moreland, K.T., Stegeman, R.A., Hood, W.F., Gierse, J.K., Stevens, A.M., Goodwin, D.C., Rowlinson, S.W., Marnett, L.J., Stallings, W.C., and Kurumbail, R.G. (2000) Structural insights into the stereochemistry of the cyclooxygenase reaction. *Nature* **405**, 97–101
36 Callan, O.H., So, O.Y., and Swinney, D.C. (1996) The kinetic factors that determine the affinity and selectivity for slow binding inhibition of human prostaglandin H synthase 1 and 2 by indomethacin and flurbiprofen. *J. Biol. Chem.* **271**, 3548–3554
37 Mancini, J.A., Riendeau, D., Falgueyret, J.P., Vickers, P.J., and O'Neill, G.P. (1995) Arginine 120 of prostaglandin G/H synthase-1 is required for the inhibition by nonsteroidal anti-inflammatory drugs containing a carboxylic acid moiety. *J. Biol. Chem.* **270**, 29372–29377
38 Rowlinson, S.W., Kiefer, J.R., Prusakiewicz, J.J., Pawlitz, J.L., Kozak, K.R., Kalgutkar, A.S., Stallings, W.C., Kurumbail, R.G., and Marnett, L.J. (2003) A novel mechanism of cyclooxygenase-2 inhibition involving interactions with Ser-530 and Tyr-385. *J. Biol. Chem.* **278**, 45763–45769
39 Kalgutkar, A.S., Crews, B.C., Rowlinson, S.W., Marnett, A.B., Kozak, K.R., Remmel, R.P., and Marnett, L.J. (2000) Biochemically based design of cyclooxygenase-2 (COX-2) inhibitors: facile conversion of nonsteroidal antiinflammatory drugs to potent and highly selective COX-2 inhibitors. *Proc. Natl. Acad. Sci. USA* **97**, 925–930
40 Komoto, J., Yamada, T., Watanabe, K., and Takusagawa, F. (2004) Crystal structure of human prostaglandin F synthase (AKR1C3). *Biochemistry* **43**, 2188–2198
41 Weber, A., Casini, A., Heine, A., Kuhn, D., Supuran, C.T., Scozzafava, A., and Klebe, G. (2004) Unexpected nanomolar inhibition of carbonic anhydrase by COX-2-selective celecoxib: new pharmacological opportunities due to related binding site recognition. *J. Med. Chem.* **47**, 550–557
42 Chen, X., Morris, K.R., Griesser, U.J., Byrn, S.R., and Stowell, J.G. (2002) Reactivity differences of indomethacin solid forms with ammonia gas. *J. Am. Chem. Soc.* **124**, 15012–15019